cannot always be realized because the ribosome does not select tRNA's paired to the correct reading frame with an equivalently high degree of accuracy, and also because messages may rephase against the anticodon stack when alternative nucleotide pairing arrangements are possible.

REFERENCES AND NOTES

1. J. R. Roth, *Cell* **24**, 601 (1981).
2. L. Bossi and J. R. Roth, *ibid.* **25**, 489 (1981).
3. L. Bossi and D. M. Smith, *Proc. Natl. Acad. Sci. U.S.A.* **81**, 6105 (1984).
4. R. F. Gaber and M. R. Culbertson, *Gene* **19**, 163 (1982).
5. ——, *Mol. Cell. Biol.* **4**, 2052 (1984).
6. N. E. Prather *et al.*, *Proc. Natl. Acad. Sci. U.S.A.* **78**, 7408 (1981).
7. E. J. Murgola *et al.*, *ibid.* **80**, 4936 (1983).
8. M. Li and A. Tzagoloff, *Cell* **18**, 47 (1979).
9. M. Yarus *et al.*, R. C. Thompson, *J. Mol. Biol.* **192**, 235 (1986).
10. G. J. Quigley and A. Rich, *Science* **194**, 796 (1976).
11. S. R. Holbrook, J. L. Sussman, W. R. Warrant, G. M. Church, S.-H. Kim, *J. Mol. Biol.* **123**, 631 (1978).
12. J. E. Ladner *et al.*, *Proc. Natl. Acad. Sci. U.S.A.* **72**, 4414 (1975).
13. M. Sundaralingam, in *Transfer RNA: Structure, Properties and Recognition*, P. Schimmel, D. Söll, J. Abelson, Eds. (Cold Spring Harbor Laboratory, Cold Spring Harbor, NY, 1979), p. 115.
14. A. J. M. Matzke, A. Barta, E. Kuechler, *Proc. Natl. Acad. Sci. U.S.A.* 77, 5110 (1980).
15. C. W. A. Pleij, K. Rietveld, L. Bosch, *Nucleic Acids Res.* **13**, 1717 (1985).
16. D. Ayer and M. Yarus, *Science* **231**, 393 (1985).
17. M. Sumner-Smith *et al.*, *Mol. Gen. Genet.* **197**, 447 (1984).
18. C. M. Cummins, M. R. Culbertson, G. Knapp, *Mol. Cell Biol.* **5**, 1760 (1985), M. Winey, M. D. Mendenhall, C. M. Cummins, M. R. Culbertson, G. Knapp, *J. Mol. Biol.* **192**, 49 (1986).
19. T. F. Donahue, P. J. Farabaugh, G. R. Fink, *Gene* **18**, 47 (1982).
20. J. F. Curran and M. Yarus, *Proc. Natl. Acad. Sci. U.S.A.* **83**, 6538 (1986).
21. Frameshift-dependent expression of the *E. coli* release factor 2 gene has been described [W. J. Craigen and C. T. Caskey, *Nature (London)* **322**, 273 (1986)].
22. Frameshift-dependent gene expression in retroviruses has been described, [D. E. Schwartz, R. Tizard, W. Gilbert, *Cell* **32**, 853 (1983); T. Jacks and H. E. Varmus, *Science* **230**, 1237 (1985); R. A. Kramer *et al.*, *ibid.* **231**, 1580 (1986); Y. Yoshinaka *et al.*, *J. Virol.* **57**, 826 (1986); R. Moore, M. Dixon, R. Smith, G. Peters, C. Dickson, *ibid.* **61**, 480 (1987)].
23. Frameshifting in yeast has been described [J. Mellor *et al.*, *Nature (London)* **313**, 243 (1985); J. Clare and P. Farabough, *Proc. Natl. Acad. Sci. U.S.A.* **82**, 2829 (1985); W. Wilson, M. H. Malim, J. Mellor, A. J. Kingsman, S. M. Kingsman; *Nucleic Acids Res.* **14**, 7001 (1986)].
24. T. Jacks, K. Townsley, H. E. Varmus, J. Majors, *Proc. Natl. Acad. Sci. U.S.A.* **84**, 4298 (1987).
25. J. F. Curran and M. Yarus, in preparation.
26. R. B. Weiss, D. M. Dunn, J. F. Atkins, R. F. Gesteland, *Cold Spring Harbor Symp. Quant. Biol.*, in press.
27. A. G. Bruce, J. F. Atkins, R. F. Gesteland, *Proc. Natl. Acad. Sci. U.S.A.* **83**, 5062 (1986).
28. C. G. Kurland, in *Nonsense Mutations and tRNA Suppressors*, J. Celis and J. D Smith, Eds. (Academic Press, New York, 1979), p. 95.
29. J. F. Atkins, D. Elseviers, L. Gorini, *Proc. Natl. Acad. Sci. U.S.A.* **69**, 1192 (1972).
30. J. Gallant and D. Foley, in *Ribosomes: Structure, Function, and Genetics*, G. Chambliss *et al.*, Eds. (University Park Press, Baltimore, 1979), p. 615.
31. R. Weiss and J. Gallant, *Nature (London)* **302**, 389 (1983).
32. ——, *Genetics* **112**, 727 (1986).
33. J. F. Atkins, R. F. Gesteland, B. R. Reid, C. W. Anderson, *Cell* **18**, 1119 (1979).
34. S. W. Cline, M. Yarus, P. Wier, *DNA* **5**, 37 (1986).
35. J. Vieira and J. Messing, *Gene* **12**, 259 (1982).
36. F. Fuller, *ibid.*, **19**, 43 (1982).

37. We thank T. Jacks, H. Varmus, R. Weiss, and E. Murgola for communications of unpublished results; we also thank T. Jacks, O. Uhlenbeck, and members of our lab group for comments on the manuscript. Supported by NSF (grant DBM-8602724 to J.F.C.) and NIH (grant GM30881 to M.Y.), for which we are grateful.

18 August 1987, accepted 4 November 1987

Star Formation in W49A: Gravitational Collapse of the Molecular Cloud Core Toward a Ring of Massive Stars

Wm. J. Welch, J. W. Dreher, J. M. Jackson, S. Terebey, S. N. Vogel

High-resolution molecular line and continuum radio images from the Hat Creek Radio Observatory and the Very Large Array suggest that the core of the W49A star-forming region is undergoing gravitational collapse. The radio continuum shows a 2-parsec ring of at least ten distinct ultracompact H-II regions, each associated with at least one O star. The ring is a region of large-scale, organized massive star formation. Recombination line velocities and HCO^+ excitation requirements indicate that the ring is rotating around 50,000 solar masses of material. Because the HCO^+ (1-0) line shows red-shifted absorption but blue-shifted emission, the molecular cloud core is believed to be collapsing toward the center of the ring. The HCO^+ radial velocities, as well as H-I, H_2CO, and magnetic-field measurements, fit a simple model of inside-out gravitational collapse of a once magnetically supported cloud.

Although it is a common expectation that stars form as a result of the collapse of molecular clouds, direct evidence of this process (*1*) is hard to find. The difficulties in finding a cloud in the stage of collapse are fourfold. First, molecular clouds are opaque to visible light, so they must be studied at infrared and radio wavelengths. Second, the time required for a cloud core to collapse (about 10^5 to 10^6 years) is small compared with the lifetimes of molecular clouds (about 10^7 to 10^8 years). Therefore, the core must be observed just as it undergoes a relatively short-lived phase in its history. Third, astronomers are limited to obtaining two-dimensional images of three-dimensional objects. Consequently, it is sometimes difficult to separate the components of a cloud that lie along the same line of sight. Finally, the small systematic

Wm. J. Welch is director and J. M. Jackson is a visiting research astronomer, Radio Astronomy Laboratory, University of California, Berkeley, CA 94720. J. W. Dreher is an associate professor of physics, Massachusetts Institute of Technology, Cambridge, MA 02139. S. Terebey is a research radio astronomer, Owens Valley Radio Observatory, California Institute of Technology, Pasadena, CA 91125. S. N. Vogel is an assistant professor of physics, Rensselaer Polytechnic Institute, Troy, NY 12181.

velocities that result from gravitational infall onto single stars are difficult to distinguish from the ever-present random motions of the gas.

Perhaps the most spectacular star-forming region in our galaxy is W49A, where a cluster of massive B and O stars [stars containing from a few to about 50 solar masses ($M_{\odot} = 2 \times 10^{33}$ g)] has recently formed. During the formation of a cluster of stars rather than a single star, the velocities that arise from gravitational collapse are expected to be larger. In the present study of the W49A star-forming region, we have measured relatively large gas velocities. Furthermore, the sources of continuum radiation in the center of the molecular cloud act as beacons that allow us to determine the position of some of the gas along the line of sight. Our observations fit a simple model of inside-out gravitational collapse, in which the collapse begins in the center of the cloud, followed by collapse at successively larger radii.

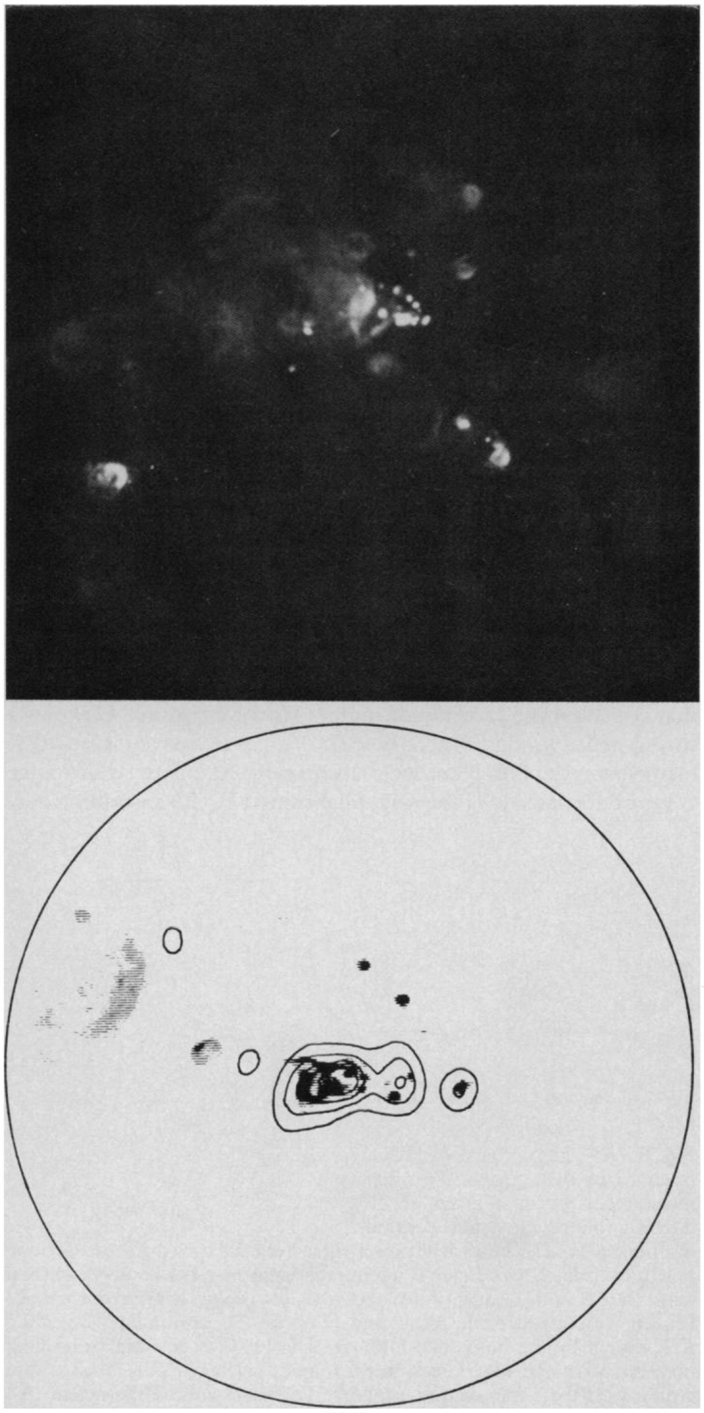

Fig. 1. (Top) An image of the core of W49A made with the VLA at 6-cm wavelength, which shows emission from ionized gas clouds, each surrounding one or more hot O stars. The ring onto which the cloud core is presently collapsing is evident in the center. (Bottom) A negative enlargement of the ring with a few contours of the 3-mm wavelength continuum map superposed. The large circle has a diameter of 42″, 3 pc at the distance of W49A.

The ionized gas (H-II) complex W49A is the most luminous in our galaxy, and the surrounding giant molecular cloud is one of the largest known, with a mass of $\approx 10^6 M_{\odot}$ (*2, 3*). It is situated at a distance of 14 kiloparsecs (1 kpc = 3×10^{21} cm) on the far side of the galaxy at about the same distance from the galactic center as the sun. Because of extremely high extinction at visible wavelengths, this region can only be studied at radio and infrared wavelengths. Previous radio continuum maps (*4–6*) showed complex distributions of ionized gas in the core, indicating a young cluster of O and B stars. Infrared observations (*7, 8*) have revealed an overall bolometric luminosity of nearly 10^7 solar luminosities ($L_{\odot} = 4 \times 10^{33}$ erg sec^{-1}). Strong H_2O maser emission with a velocity spread of nearly 500 km sec^{-1} (*9, 10*) and bipolar flows (*11, 12*) provide evidence that star formation is still in progress.

Radio maps from Hat Creek and the Very Large Array. We have observed W49A with the Very Large Array (VLA) (*13*) at 6-cm wavelength in the A, B, C, and D configurations. Employing the usual CLEAN and self-calibration algorithms, which correct the image for the incomplete aperture of an interferometer and errors in calibration, respectively, we made radio maps that cover a field of more than 10′ with an angular resolution of 0.4″, while maintaining response to structures up to a few arc minutes across. We have also mapped the H76α recombination line at 2 cm in the C array with an angular resolution of 1.2″ and spectral resolution of 3 km sec^{-1} (*14*).

Both continuum and molecular line maps have been made at 3-mm wavelength with the Hat Creek Interferometer (*15*). Here we discuss HCO^+ (1-0) observations. The continuum map has a resolution of 2.5″ and is sensitive to structures up to 20″ in diameter over a field of 2′. The HCO^+ maps have a spectral resolution of 2.1 km sec^{-1}, an angular resolution of 7″, and are sensitive to structures up to about 45″ in size (*16*).

The rotating 2-parsec ring of H-II regions. The 6-cm continuum map of the core of the ionized gas complex shows a remarkable ring of compact H-II regions in the center (Fig. 1, top). The 3-mm wavelength continuum emission coincides with the brightest H-II regions in the ring (Figure 1, bottom; for reference, the circle has a diameter of 42″, 3 pc at the distance of W49A). The ring lies at the center of the cloud core and contains about ten distinct ionized regions, ranging in size from about 0.01 pc to 0.5 pc. Although shock heating could conceivably explain the ionized gas clumps, their sharp edges, their uniform brightness temperatures of about 8000 K at long wavelengths, and their continuum spectra (*6*) are more naturally explained as gas photoionized by hot stars. Further, from the intensity of the continuum emission the total luminosity of the ionizing stars can be estimated, and this luminosity roughly agrees with the observed total luminosity of the region (*6*). We therefore conclude that each H-II region contains at least one O star; some clearly contain more than one star (*14*).

From our observations of the H76α recombination line, we can find the radial velocity of each H-II region. (The exception is the westernmost H-II region, whose intrinsic linewidth exceeds the width of the passband.) The average systemic velocity of the ring is 8 ± 2 km sec^{-1}, in good agreement with the velocity of 7.5 km sec^{-1} from lower angular resolution H109α observations (*17*) and 6.3 ± 0.1 km sec^{-1} from H66α observations (*18*). The radial velocities of the H-II regions in the ring clearly vary monotonically with position (Fig. 2). If all the H-II regions rotate on a circle, the

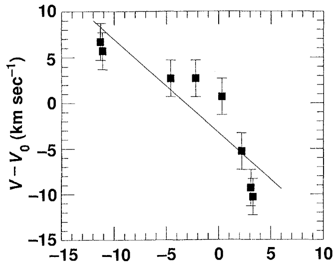

Fig. 2. The mean measured radial velocities of the H76α recombination line emitted by the ionized gas of each of the compact H-II regions in the ring. The velocity is relative to the mean of 8 km sec^{-1}. The abscissa is arc seconds along the right ascension coordinate relative to the 3-mm wavelength peak.

radial velocities should change linearly with projected distance along the major axis. Deviations from a straight line may indicate a noncircular geometry, random motions of the clumps, or motion of gas within the individual clumps. The simplest interpretation of Fig. 2 is that the ring is rotating at an apparent angular velocity of 13 km sec^{-1} pc^{-1}. Assuming the ring to be a true circle seen at an inclination angle of 65°, we correct the angular velocity to 14.4 km sec^{-1} pc^{-1}.

The diameter of the ring is 2 pc, and if, as seems likely, it is in centrifugal equilibrium, the mass included within the ring is about $5 \times 10^4\ M_\odot$. This estimate is consistent with the observation of HCO^+ within and around the ring. Collisional excitation of HCO^+ requires a density of $\geq 3 \times 10^5$ hydrogen molecules per cubic centimeter. A disk of this density, 2 pc in diameter and 1.0 pc in height, a flattened structure consistent with the observed rotation, has the same mass. A similar mass for the cloud core has been found from 1300-μm continuum, $C^{18}O$ (2-1), and CS (2-1) observations (*19, 20*).

The HCO^+ (1-0) observations: Evidence for a collapse. HCO^+ (1-0) has been observed toward the ring in W49A at 42″ angular resolution (corresponding to the circle superposed on Fig. 1, bottom) with the Onsala Millimeter Wave Telescope (*21*) (Fig. 3A). For comparison, we present the HCO^+ spectrum in a 12″ beam centered on the 3-mm continuum maximum observed with the Hat Creek interferometer (Fig. 3B). The absorptions near 40 km sec^{-1} and 60 km sec^{-1} are the same in both spectra. The emission over the range −10 to +30 km sec^{-1} in both spectra comes principally from a region of about 3-pc diameter approximately centered on the ring (*22*).

We interpret the minimum at 7 km sec^{-1}, especially prominent in the Onsala spectrum, as absorption by cold gas in the outer envelope of the molecular cloud. This dip, dividing the emission in two, is apparent in CO (1-0) and CS (1-0) spectra of W49 and has been interpreted by some workers as evidence for two distinct clouds (*2, 3, 20*). However, the emission spectra of the SiO (1-0, $v = 0$), the less abundant $H^{13}CO^+$ (1-0) (Fig. 4), and of the higher excitation CO lines that are absent in the cold outer parts of the cloud show broad lines with single emission peaks near 7 km sec^{-1} (*16, 22–24*). Further, because the velocity of the dip agrees with the systematic velocity of the 2-pc ring, this feature is almost certainly caused by absorption by envelope gas at the local systemic velocity.

The critical evidence for collapse is the asymmetry in the HCO^+ absorption and emission. Whereas the Onsala spectrum shows only weak absorption over the range 16 to 18 km sec^{-1}, the Hat Creek spectrum exhibits deep absorption from 11 to 21 km sec^{-1} (Fig. 3). The difference occurs because, for absorption, the line excitation temperature must be less than the continuum brightness temperature, averaged over the beam; the continuum brightness temperature is much higher in the interferometer spectrum because of smaller beam dilution. The absorption is clearly red-shifted relative to the systemic velocity of 7 km sec^{-1}, whereas the blue-shifted gas is entirely in emission. This shows that gas both on the near side of the continuum source (seen in absorption) and on the far side (seen in emission) is moving toward the continuum source.

To demonstrate that the absorption is not just in a small localized cloud in front of the strong 3-mm continuum source, we show HCO^+ (1-0) interferometer spectra in other directions in Fig. 4. Wherever there is 3-mm continuum (see Fig. 1, bottom), however weak, there is clear absorption in the 11 to 21 km sec^{-1} range. Where the continuum is weak or absent, there is an absence of HCO^+ emission, consistent with self-absorption. Thus, the spatial extent of the 11 to 21 km sec^{-1} absorption is over the entire ring. To be certain that this gas is local to the core and not a distant foreground absorption, we summarize other observations of W49A.

Other spectral observations. H_2CO (*25*) and H-I (*26*) have been observed toward both W49A and the supernova remnant W49B, which is only 12′ to the east of W49A. In both of these lines, there is essentially no absorption seen toward W49B over 0 to 20 km sec^{-1}, whereas there is strong absorption toward W49A at these velocities, especially in the direction of the ring. Because W49A and W49B are so close in angle (and therefore probably at the same distance), these results indicate that the 0 to 20 km sec^{-1} gas is local to the W49A cloud (*27*), and that the HCO^+ absorption at 11 to 21 km sec^{-1} is also local to W49A. In contrast, the spectral features at 40 and 60 km sec^{-1}, evident in the HCO^+ spectra, are also apparent in H_2CO and H-I toward W49B. These components are thus in the foreground and are probably associated with the Sagittarius spiral arm (*27*).

Absorption in the 6-cm transition of H_2CO (*28*) and in the (2, 2) and (3, 3) transitions of NH_3 (*16*) has been observed toward the compact H-II regions in W49A at high angular resolution, with absorption features over 5 km sec^{-1} to 20 km sec^{-1}. This is just the velocity range expected if this gas is part of the proposed infall. H_2CO absorption is also observed over 0 to 5 km sec^{-1} toward one of the H-II regions in the ring, source G (*6*). In our picture, this part of the spectrum should correspond to the portion of the infalling gas that is behind the continuum source. However, source G shows a strong stellar wind (*16*) with blue-shifted gas in front of it, and that may explain the 0 to 5 km sec^{-1} absorption. Alternatively, if source G lies on the far side of the ring, blue-shifted H_2CO absorption may

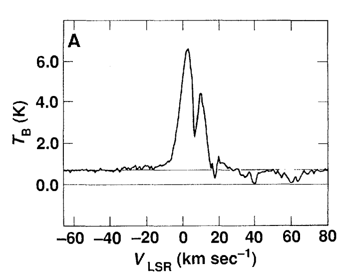

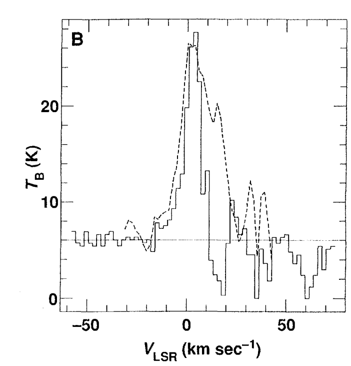

Fig. 3. (**A**) The spectrum of HCO^+ observed by the Onsala 20-m millimeter telescope in a beam of 42″ directed toward the 3-mm continuum peak (*21*). The beam half-power diameter corresponds to the circle in Fig. 1, bottom. The ordinate is intensity in equivalent blackbody brightness temperature. The frequency scale of the abscissa is converted to radial velocity with respect to the local standard of rest. The continuum level at 0.7 K is shown by the horizontal line. (**B**) The HCO^+ spectrum (solid line) observed with the Hat Creek interferometer averaged over a 12″ beam centered on the 3-mm continuum peak. The scales are the same as in (A). The continuum level is 6 K here. The absorptions at 40 and 60 km sec^{-1} in both spectra are probably formed in foreground galactic spiral arms. The main difference between the spectra is the strong, broad absorption over 11 to 21 km sec^{-1} in the Hat Creek data. Superposed on the HCO^+ (1-0) spectrum is the CO (7-6) spectrum (dashed line) (*24*). For clarity, the CO (7-6) brightness temperature has been reduced by 30%, within the calibration errors for either spectrum.

be seen if the infall continues past the ring. The detection of both NH_3 (2, 2) and NH_3 (3, 3) absorption is particularly significant, because they require molecular hydrogen densities of 5×10^3 cm^{-3} or more to populate these levels, and such densities are not expected in diffuse foreground clouds.

Jaffe, Harris, and Genzel (*24*) have observed CO (7-6) emission toward W49A with an angular resolution of 30″, finding an extent similar to that of HCO^+. The dashed curve in Fig. 3B is their central spectrum. Toward the strongest 3-mm continuum source the two molecules have about the same brightness in emission at all velocities, except for the 11 to 21 km sec^{-1} absorption in the HCO^+ spectrum. Since the CO (7-6) transition has a radiative lifetime and collisional excitation rate very like that of the HCO^+ (1-0) transition, in the cloud core where the densities and optical depths are high the emission spectra should agree, as observed. However, the $J = 6$ CO level lies about 100 K above the ground state, whereas the $J = 0$ level of HCO^+ is the ground state for that molecule. The absence of CO (7-6) absorption is expected because in the lower density foreground gas no CO is excited to the $J = 6$ level, whereas HCO^+ in the $J = 0$ level is present there.

An alternative explanation: two clouds colliding. Besides collapse, the only other obvious interpretation of the data is that the star formation is the result of two clouds colliding along the line of sight. Although this possibility cannot be entirely ruled out, it is improbable. The two peaks in the CO (1-0) and CS (1-0) spectra are clearly due to self-absorption. Since there is no evidence for a spatial separation into two clouds in any of the data, the clouds would have to be well aligned along the line of sight, an unlikely special geometry. Note that the average velocity dispersion for molecular clouds in the galaxy is about 5 km sec^{-1} (*29*). The root-mean-square velocity for random collisions would then be about 7 km sec^{-1}. The difference between the average HCO^+ emission and absorption velocities in W49A is 13 km sec^{-1}, substantially greater than 7 km sec^{-1}, which means that a random collision is unlikely. Finally, in the cloud collision model, the foreground cloud velocities must, by coincidence, exactly mimic the free-fall collapse velocities. We favor the simpler collapse model that naturally explains the range of absorption velocities of the HCO^+ and other molecular lines as well as the observed cloud structure.

An inside-out collapse picture. Because of the evident increase in concentration of material toward the ring and the kinematic evidence for large-scale collapse, it is natural to assume that an inside-out collapse is in progress, producing not one but a cluster of massive stars. In the inside-out collapse picture, the initial state is a marginally stable, centrally condensed cloud core. Collapse begins in the center, and the region of collapse expands outward at the sound speed. In the case of an unmagnetized, nonrotating cloud, the central radial velocity distribution approaches free-fall, $V(R) \propto R^{-0.5}$, and the material falls onto a spherical accretion shock (*30*).

Although theoretical investigations of inside-out collapse have heretofore considered only the collapse of single stars, we suggest that the inside-out collapse picture also applies to the formation of the massive star cluster in the core of W49A. We presume the center of collapse to be the center of the ring of O stars. The accretion shock lies outside the ring; we take its boundary to be the extent of the HCO^+ emission, a diameter of about 3 pc. The time scale and the large spatial scale require an effective sound speed that greatly exceeds the isothermal sound speed. We argue that magnetic Alfvén waves have the proper speeds, and that magnetic fields play an important role in the collapse. We summarize below kinematic evidence and present a detailed discussion of this collapse picture for W49A.

Kinematic evidence for inside-out gravitational collapse. The simplest interpretation of the HCO^+ observations is that the inner envelope of the giant molecular cloud is in free fall toward the 2-pc ring of H-II regions. In the few parsecs exterior to the accretion shock, the velocity field is fixed only by the mass interior to the shock. For the 50,000 $M_\odot$ core of W49A, this field is $V(R) = 21 \times R^{-0.5}$, with V in km sec^{-1} and R in parsecs.

The 3-mm continuum emission from W49A is primarily from a source displaced from the ring center by about 1 pc in the plane of

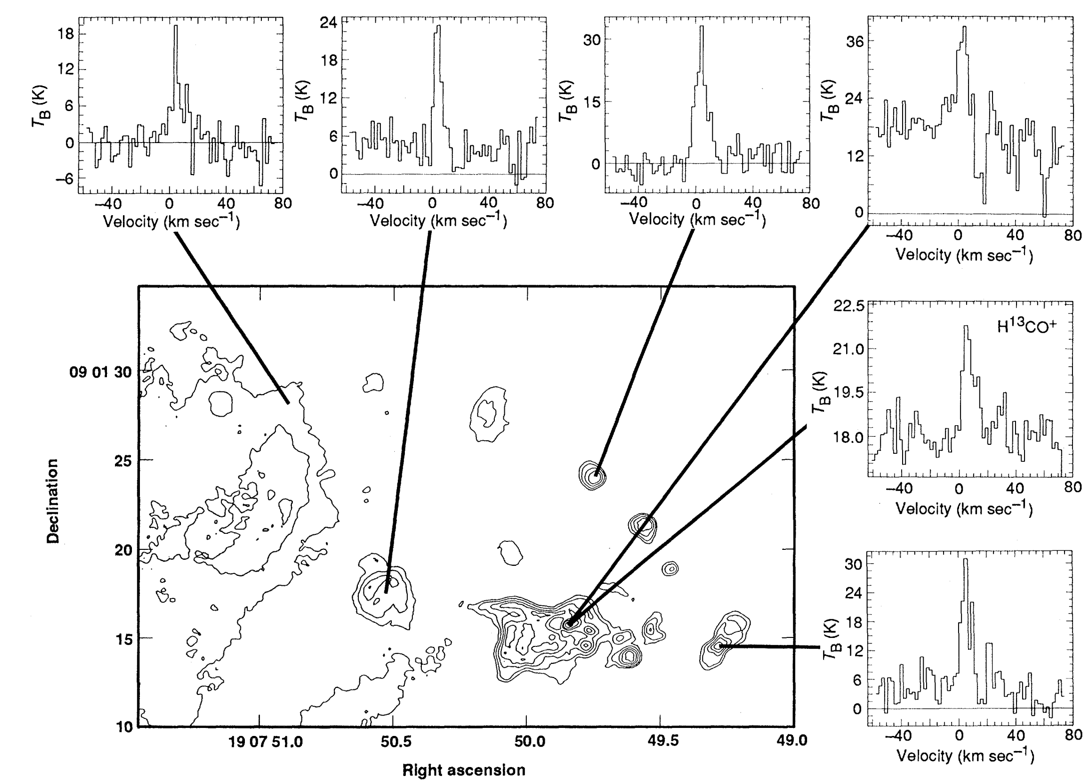

Fig. 4. Spectra of HCO^+ and $H^{13}CO^+$ (1-0) emission toward several positions of the ring, represented here by the VLA 6-cm continuum map. The HCO^+ spectra have an angular resolution of 6″; the $H^{13}CO^+$ spectrum has an angular resolution of 12″; and the continuum map has an angular resolution of 0.4″. The spectra present the beam diluted brightness temperature of the HCO^+ and $H^{13}CO^+$ lines versus the radial velocity with respect to the local standard of rest. In the continuum map, the contour levels are 2.5, 5, 10, 15, 20, and 30 mJy per beam. Note that the absorption is absent in the $H^{13}CO^+$, because of its lower abundance. The lack of HCO^+ emission in the range 11 to 21 km sec^{-1} is consistent with the absorbing gas lying in front of the entire ring.

the sky (Fig. 1, bottom), and the HCO^+ absorption therefore occurs along a ray toward this source. The observed radial velocity is the projection of the collapse velocity onto this ray. Near the source, the observed velocity increases with distance because of projection effects, but farther out the radial decrease in collapse velocity dominates and the observed velocity falls; the maximum projected velocity is reached at a radius of several parsecs. Given our assumed geometry for the ring, the maximum velocity seen toward the continuum source should be 14 km sec^{-1} higher than the systemic velocity. Note the cutoff in the observed absorption at 21 km sec^{-1}, just 14 km sec^{-1} higher than the systemic velocity of 7 km sec^{-1}, as expected.

We do not observe significant changes in the maximum velocities of HCO^+ absorption toward the 3-mm continuum sources. This is consistent with the small range in projected distance from the center of collapse to the 3-mm continuum sources.

Two effects are ignored in our simple dynamical model. First, we have not treated the angular momentum of the infalling gas, which the presence of the rotating ring shows must eventually affect the gas streamlines. Second, we have not taken into account the distributed nature of the core mass, and this can change the gravitational potential. However, at distances larger than the ring radius r_d both effects rapidly decrease in importance. The main result of including angular momentum is to change the direction, but not the magnitude, of the gas velocity along a streamline. The maximum line-of-sight velocity toward the continuum source comes from gas at about $2r_d$, and at this distance the inclusion of angular momentum produces a $\leq 33\%$ change in the maximum observed velocity (*31*). It is harder to judge the importance of the second effect, because we do not know the mass profile of the ring and envelope, but there is not likely to be a large change in the gas velocity at a distance $2r_d$ from the ring. We therefore conclude that the inclusion of angular momentum and a nonspherical mass distribution can affect the quantitative but not the qualitative interpretation provided by the simple dynamical model.

Importance of magnetic fields. Analytic models of inside-out collapse for nonrotating, gravitationally dominated material predict a constant mass flow, $\dot{M}$, onto the central core at the rate a^3/G, where a is the sound speed and G is the gravitational constant (*30*). We can estimate $\dot{M}$ from the observations by $\dot{M} = 2\pi r^2 \rho v$. The particle density of the infalling gas outside the shock must be $10^{4\pm1}$ cm^{-3} to be consistent with the observed molecular excitation, and the radial velocity at the shock is the free-fall velocity, 20 km sec^{-1}. The mass accretion rate is then of order $10^{-1\pm1}$ $M_\odot$ per year. The implied time scale of about 10^6 years is sensible for the formation of massive stars. The derived sound speed, a, is 5 to 10 km sec^{-1}.

The coherent formation of stars in the rotating ring also suggests that the effective sound speed must be on the order of 14 km sec^{-1}, the rotational speed of the ring, in order to coordinate the star formation. Altogether, the required effective sound speed must be of the order of 10 km sec^{-1}, but this is larger than the isothermal sound speed by more than an order of magnitude. If, however, magnetic fields play an important role in the cloud dynamics, the Alfvén speed may be the effective sound speed. An Alfvén speed of 10 km sec^{-1} for densities 10^5 cm^{-3} requires a magnetic field of about 2 mG.

In fact, such large magnetic fields have been measured near the H-II regions in the ring. The observation of Zeeman splitting of OH maser lines implies fields of the order of 3 to 9 mG toward several positions (*32*). Since the cloud core is over 1000 times larger than a typical maser, it is not known if the magnetic field measured toward a maser reflects the prevailing large-scale field. However, the densities of OH masers can be no larger than about 10^7 cm^{-3} (*33*), only a factor of 100 greater than the average density in the cloud core. Since the magnetic field increases only weakly with density, $B \propto n^\beta$, where $\beta = 0.3$ to 0.5 (*34*), the magnetic fields in the cloud core are probably on the order of 1 mG or more.

In addition to providing high effective sound speeds, magnetic fields may also have played a critical role in the cloud evolution before collapse. The fields may delay the collapse of the cloud until a large critical mass is reached, providing the large pool of material for high-mass star formation (*30*).

A rotating gaseous disk. The rotation of the ring of H-II regions shows that the infalling material has significant angular momentum, and it is likely that the core has collapsed into a flattened disk rather than a sphere. The rotational period of this disk, T_d, inferred from the recombination line observations, is 4×10^5 years. Evolution of the disk should proceed on this time scale unless the disk is violently unstable when it forms. The striking pattern found in the O stars suggests a wave origin, which would require a disk age of one period or longer for wave instabilities to grow and develop. The persistence of the O star ring is consistent with a disk near stability since a random velocity imparted to the O stars of as little as 5 km sec^{-1} would destroy the pattern in one period. However, since random velocities of this order may exist (Fig. 2), the ring could disperse in a few orbital periods.

The accretion shock. When the infalling molecular envelope nears the disk, it is moving at a free-fall velocity, v_f, of about 20 km sec^{-1}. Because the speed of the infalling gas exceeds both the isothermal sound speed and the Alfvén velocity, it passes through a standing shock before becoming incorporated into the disk. In most astrophysical situations, the post-shock gas is able to cool easily, allowing the gas to reach high compression ratios, but a magnetic field can limit the maximum compression. We estimate the significance of this effect by assuming a field parallel to the shock front and equating the preshock ram pressure $\rho_0 v_f^2$ to the post-shock magnetic energy density $B_1^2/8\pi$. Here ρ_0 is the preshock molecular hydrogen density and B_1 is the post-shock magnetic field. A field, B_1, of 3 mG and a velocity, v_f, of 20 km sec^{-1} give a preshock molecular hydrogen density, ρ_0, of 2.5×10^4 cm^{-3}. Thus in the most favorable geometry a magnetic field of 3 mG could limit the compression to a factor of four. Since the orientation of the field is likely to be at some angle with respect to the shock front, a factor of ten is likely a more characteristic value for the compression and concomitant change in the field strength across the shock. This gives an estimated preshock density and magnetic field of 10^4 cm^{-3} and 300 μG, respectively. Note that the lack of self-absorption in the CO (7-6) line requires an abrupt decrease in density in front of the cloud core (*24*), consistent with our model shock.

With this preshock density estimate, the reasonable assumption that the simple free-fall velocity distribution holds where the HCO^+ absorption line forms, and the observed optical depth of about 2 (Fig. 3B), we can estimate the fractional abundance of HCO^+ (*16*). The derived value of about 10^{-9} HCO^+/H_2 is typical of the HCO^+ abundance in molecular clouds (*20*). This supports the notion that the HCO^+ absorption is produced in an extended, collapsing envelope.

We can now better estimate the mass accretion rate onto the disk as $\dot{M} = 2\pi r_d^2 \rho_0 v_f = 0.07$ $M_\odot$ per year. The luminosity radiated from the shock will be of the order of $\dot{M} v_f^2 = 4500$ $L_\odot$.

The ratio $M_d/\dot{M} = 7 \times 10^5$ years gives an estimate of the time T_c required to build the disk. In the specific case of inside-out collapse models where the cloud core is initially near equilibrium and the inside collapses first, the time T_c is almost exactly the time since onset of collapse (*31*). This age is consistent with our previous argument that the disk is older than one rotation period.

Conclusions. Our high-resolution studies of W49A with the VLA and the Hat Creek millimeter interferometer reveal two important large-scale properties of this region of massive star formation. First, the 2-pc ring of H-II regions demonstrates, for the first time, that the formation of massive stars can occur coherently over large scales. Second, the rotation of this ring and the HCO^+ line emission and absorption profile strongly suggest that we are seeing the collapse of the core of the W49A molecular cloud onto a warm, dense, rotating disk of molecular gas. This disk has a mass of 50,000 $M_\odot$ and a density greater than 10^5 cm^{-3}.

The primary evidence for infall is the presence of red-shifted absorption (seen against the embedded continuum sources) and blue-shifted emission. The velocities of these features are just those appropriate for the mass and size of the disk. In addition, the absence of the absorption feature in $H^{13}CO^+$ and CO (7-6) is consistent with this simple infall picture, since the former should have insufficient optical depth to show marked absorption and the latter has a ground state that is too high to be excited in a cool infalling envelope. None of these facts are consistent with the "two-cloud" model. Consideration of the physical conditions suggests a semiquantitative "inside-out" collapse model. In this scenario the infalling envelope, with $n \approx 10^4$ cm^{-3}, passes through an accretion shock at $r \approx 1$ pc. The density jump through the shock is limited by a magnetic field to be around ten. The accretion rate is ≈ 0.1 $M_\odot$ per year. This model requires an Alfvén velocity of 5 to 10 km sec^{-1}; within the disk the magnetic field must then be ≈ 3 mG.

The basic kinematic collapse picture seems to us to be nearly unavoidable. Naturally, the more detailed "inside-out" model is somewhat speculative, but there are testable predictions. Maps of molecular lines with energy levels well above the ground state or requiring densities greater than 10^4 cm^{-3} for excitation will be free of the absorption associated with the infall and will reveal the structure of the disk. Since the 11 to 21 km sec^{-1} gas is local to the 2-pc ring region, it should not be seen toward W49S, the H-II region to the lower left of Fig. 1, bottom. If the large-scale collapse that we have observed in W49A is indeed the principal mechanism for OB cluster formation, it should be seen toward other forming clusters. We have begun a search toward other regions that show massive molecular cores and found a similar red-shifted HCO^+ absorption feature toward W51. The "inside-out" model makes an extra prediction. There should be a $\approx$3 mG field in the disk. Such a large field can be expected to produce an observable Zeeman effect in the 21-cm neutral hydrogen line. Theoretical studies of large-scale collapse that treat both magnetic fields and rotation are needed to provide further predictions (*35*).

Although it seems certain that stars form as a result of the collapse of molecular clouds, so far the evidence for gravitational collapse has been elusive and controversial. Since OB stars tend to form in clusters, it is natural to speculate that the large-scale collapse of giant molecular clouds produces these clusters. If the collapse proceeds rapidly, as our observations suggest, the isothermal sound speed is far too small for the collapse to propagate through the cloud in the necessary times. Only magnetic Alfvén waves seem to have the proper speeds. We suggest that the collapse in W49 is typical of the formation of massive star clusters, and that magnetic fields play an important role in the collapse.

REFERENCES AND NOTES

1. P. T. P. Ho and A. Haschick, *Astrophys. J.* **304**, 501 (1986); C. K. Walker, C. J. Lada, E. T. Young, P. R. Maloney, B. A. Wilking, *ibid.* **309**, L47 (1986); E. Keto, P. T. P. Ho, A. D. Haschick, *ibid.* **318**, 712 (1987).
2. N. Z. Scoville and P. M. Solomon, *ibid.* **180**, 31 (1973).
3. S. L. Mufson and H. S. Liszt, *ibid.* **232**, 451 (1977).
4. C. G. Wynn-Williams, *Mon. Not. R. Astron. Soc.* **151**, 397 (1971).
5. N. H. Dieter, W. J. Welch, M. C. H. Wright, *Astrophys. J.* **283**, 768 (1979).
6. J. W. Dreher, K. J. Johnston, W. J. Welch, R. C. Walker, *ibid.*, p. 632.
7. E. E. Becklin, G. Neugebauer, C. G. Wynn-Williams, *Astrophys. Lett.* **13**, 147 (1973).
8. P. M. Harvey, M. H. Campbell, W. F. Hoffman, *Astrophys. J.* **211**, 786 (1977).
9. R. C. Walker, K. L. Johnson, B. F. Burke, J. H. Spencer, *ibid.*, p. L135.
10. M. Morris, *ibid.* **210**, 100 (1976).
11. N. Z. Scoville *et al.*, *ibid.* **303**, 416 (1986).
12. W. J. Welch, J. Dreher, J. M. Jackson, S. N. Vogel, S. Terebey, in *Proceedings of the 115th Symposium of the International Astronomical Union on Star Forming Regions*, M. Peimbert and J. Jugaku, Eds. (Reidel, Dordrecht, 1985), p. 143.
13. The Very Large Array is part of the National Radio Astronomy Observatory, which is operated by Associated Universities, Inc., under contract with the National Science Foundation. See also P. J. Napier, A. R. Thompson, R. D. Ekers, *Proc. IEEE* **71**, 1295 (1983).
14. J. W. Dreher, W. J. Welch, J. M. Jackson, K. J. Johnston, in preparation.
15. W. J. Welch and D. Thornton, paper presented at the URSI Symposium on Millimeter and Submillimeter Wave Astronomy, Granada (1985).
16. W. J. Welch, J. W. Dreher, J. M. Jackson, S. N. Vogel, S. Terebey, in preparation.
17. J. H. van Gorkom, W. M. Goss, P. A. Shaver, U. J. Schwartz, R. H. Harten, *Astron. Astrophys.* **89**, 150 (1980).
18. T. L. Wilson, J. Bieging, W. E. Wilson, *ibid.* **71**, 205 (1979).
19. F. P. Schloerb, R. L. Snell, P. R. Schwartz, *Astrophys. J.* **319**, 426 (1987).
20. R. Miyakawa, M. Hayashi, T. Hasegawa, *ibid.* **305**, 353 (1986).
21. L. A. Nyman, *Astron. Astrophys.* **120**, 307 (1983).
22. J. W. Dreher, W. J. Welch, J. M. Jackson, S. N. Vogel, S. Terebey, in preparation.
23. T. G. Phillips *et al.*, *ibid.* **245**, 512 (1981).
24. D. T. Jaffe, A. I. Harris, R. Genzel, *ibid.* **316**, 231 (1987).
25. J. H. Bieging, T. L. Wilson, D. Downes, *Astron. Astrophys. Suppl.* **9**, 607 (1982).
26. V. Radharkrishnan, W. M. Goss, J. D. Murray, J. W. Brooks, *Astrophys. J. Suppl.* **24**, 49 (1972).
27. P. G. Mezger, J. Schraml, Y. Terzian, *Astrophys. J.* **150**, 807 (1967).
28. H. R. Dickel, W. M. Goss, A. H. Rots, in (*12*), p. 171.
29. D. L. Sanders, P. M. Solomon, N. Z. Scoville, *Astrophys. J.* **276**, 182 (1984).
30. F. H. Shu, F. Adams, S. Linzano, *Annu. Rev. Astron. Astrophys.* **25**, 23 (1987).
31. P. Cassen and A. Moosman, *Icarus* **48**, 353 (1981); S. Terebey, F. H. Shu, P. Cassen, *Astrophys. J.* **286**, 529 (1984).
32. K. J. Johnston and S. S. Hanson, *Astron. J.* **87**, 803 (1982); R. A. Gaume and R. L. Mutel, *Astrophys. J. Suppl.* **65**, 193 (1987).
33. M. J. Reid and J. M. Moran, *Annu. Rev. Astron. Astrophys.* **19**, 231 (1981).
34. C. Heiles, in *Interstellar Processes*, D. J. Hollenbach and H. A. Thronson, Jr., Eds. (Reidel, Dordrecht, 1987).
35. T. Ch. Mouschovias, in *Protostars and Planets*, T. Gehrels, Ed. (Univ. of Arizona Press, Tucson, 1978), p. 209; P. Bodenheimer and D. C. Black, *ibid.*, p. 288.

36. This work was supported by NSF grant AST 84-16177.

27 May 1987; accepted 28 October 1987